Soils and Rocks
www.soilsandrocks.com
An International Journal of Geotechnical and Geoenvironmental Engineering
ISSN 1980-9743
ISSN-e 2675-5475

Experimental study on particle size effect on mechanical behaviour of dense calcareous sand

Du-min Kuang[1], Zhi-lin Long[1,#], Jie Wang[1], Xu-tong Zhou[1], Piao-yi Yu[1]

Article

Keywords
Calcareous sand
Particle size
Triaxial test

Abstract
To investigate the effect of particle size on mechanical properties of calcareous sand, a series of consolidated drained triaxial tests were performed on calcareous sand with different particle sizes. At a low effective confining pressure of 50 kPa, the shear peak strength increases with the increasing particle size. However, under a relatively large effective confining pressure (≥ 200 kPa), the shear peak strength decreases with the increasing particle size. Moreover, the apparent cohesion increases, and the corresponding friction angle decreases with the increase of particle size. The softening and dilatancy coefficient were proposed to evaluate the softening and dilatancy behaviour quantitatively. Calcareous sands with larger particle size show the greater strain hardening and volumetric contraction behaviour, which is more susceptible to the effective confining pressure.

1. Introduction

Calcareous sand, which is primarily composed of remains of coral and snail, is largely located in tropical or subtropical areas around the world, such as South China Sea, Red Sea, the Hormuz Island and the Persian Gulf (Coop et al., 2004; Morsy et al., 2019; Shahnazari et al., 2016; Suescun-Florez & Iskander, 2017; Wang and Jiao, 2011). In ocean geotechnical engineering, calcareous sands are commonly used as the backfill material for road embankments or airport runways (Wang et al., 2011; Xiao et al., 2019). As an essential part of construction material, the physical and mechanical properties of calcareous sand have attracted increasing research attention. The character of calcareous sands is quite different from that of terrigenous sands, exhibiting the irregular particle shape, the high Calcium carbonate content, and the large internal voids (Liu et al., 2019; Mcdowell & Bolton, 2000). As a result of these special physical properties, calcareous sands exhibit typical characteristics such as costly saturation (Lade et al., 2009), large strains to failure (Wei et al., 2018), high compressibility (Yang et al., 2017), and a dilative behaviour at low relative densities (Hyodo et al., 1998; Wang & Zhu, 2018). For granular materials, it is widely acceptable that the particle size effect can affect the mechanical properties significantly. A large number of studies for particle size effect of granular materials have been reported. Generally, the shear strength of particle assemblies increases with the increase in elementary particle size (Dadkhah et al., 2010; Wen et al., 2018; Varadarajan et al., 2003). Although there have been a few works that have addressed the mechanical properties of calcareous sand including shearing characteristics (Desrosiers et al., 2002; Salehzadeh et al., 2006; Pham et al., 2017; Zhang et al., 2018), compression characteristics (Yang et al., 2017) and hydraulic characteristics (Wang et al., 2019; Xiao et al., 2018), most of them have not focus on the particle size effect of calcareous sand. In practical engineering, the particle sizes of calcareous sands are in the range of some millimetre to some dozen-millimetres. For a comprehensive understanding of the engineering characteristics of calcareous sands, it is significant to analyse the effect of particle size on mechanical properties of calcareous sands.

In this study, a series of consolidated drained triaxial tests for calcareous sand with different particle sizes were performed. Based on the experimental results, the effect of particle size on strain-stress responses and volumetric responses were obtained. Moreover, the apparent cohesion and friction angle based on the Mohr-Coulomb failure criterion for different particle sizes were further analysed. Furthermore, the empirical softening index and dilatancy index were proposed to evaluate the effect of particle size on strain softening and dilatancy quantitatively.

#Corresponding author. E-mail address: longzl@xtu.edu.cn.
[1]College of Civil Engineering and Mechanics, Xiangtan University, Xiangtan, PR China.

Submitted on December 19, 2019; Final Acceptance on June 10, 2020; Discussion open until March 31, 2021.
DOI: https://doi.org/10.28927/SR.434567

2. Materials and methodology

The calcareous sand used in this study was obtained from Nansha islands in south of China. The calcareous sand particles own irregular and angular appearance which contains numerous cavities. Six groups of calcareous sand with particle sizes of 5-2 mm (G1), 2-1 mm (G2), 1-0.5 mm (G3), 0.5-0.25 mm (G4), 0.25-0.075 mm (G5), and 0.075-0 mm (G6) were adopted by sieving, as shown in Figure 1. Following the standards JTG E40-2007 (RIOH, 2007), the specific gravities (G_s) and the maximum (ρ_{max}) and minimum (ρ_{min}) dry densities of six particle size groups of calcareous sand are tabulated in Table 1.

The mode SLB-1 stress strain controller triaxial shear permeation test apparaus used in this study. The maximum axial pressure of this apparatus is 600 kN. The measuring capcacity of confining pressure, back pressure, and pore pressure are all 3 MPa with a resolution of 1 kPa.

In the following traxial tests, the conventional samples with 39.1 mm in diametr and 80 mm in height were assembled by the same relative density of 70 % for different particle size groups. The saturation process was conducted by the method of water head staturation combined withg back pressure saturation suggested by Yang et al. (2018). The samples are considered to be fully saturated when the Skempton's parameter B is greater than 0.95. Following this step, the samples were isotropically consolidated under different effective confining pressures of 50, 200, 400, and 800 kPa. Finally, all samples were sheared at a specific axial loading rate of 0.1 mm/min. It should be noted that all the tests were performed under drained conditions.

3. Results and discussions

3.1 Effect of particle size on stress-strain responses

Figure 2 shows the stress-strain responses of calcareous sand samples with different particle sizes under various effective confining pressures. At a low effective confining pressure (σ_3 = 50 kPa), the calcareous sand samples for different particle sizes exhibit slight strain softening behaviour, which is consistent with the shear behaviour of dense quartz sand. However, as the effective confining pressure increases (≥ 200 kPa), the samples with particle size ranging from 5 (G1 sand) to 0.25 mm (G4 sand) exhibit strain hardening behaviour. Similar results have also been reported by Hyodo et al. (1998). They suggested that the strain softening can be suppressed by the particle breakage induced by the high stress level, leading to a strain harden-

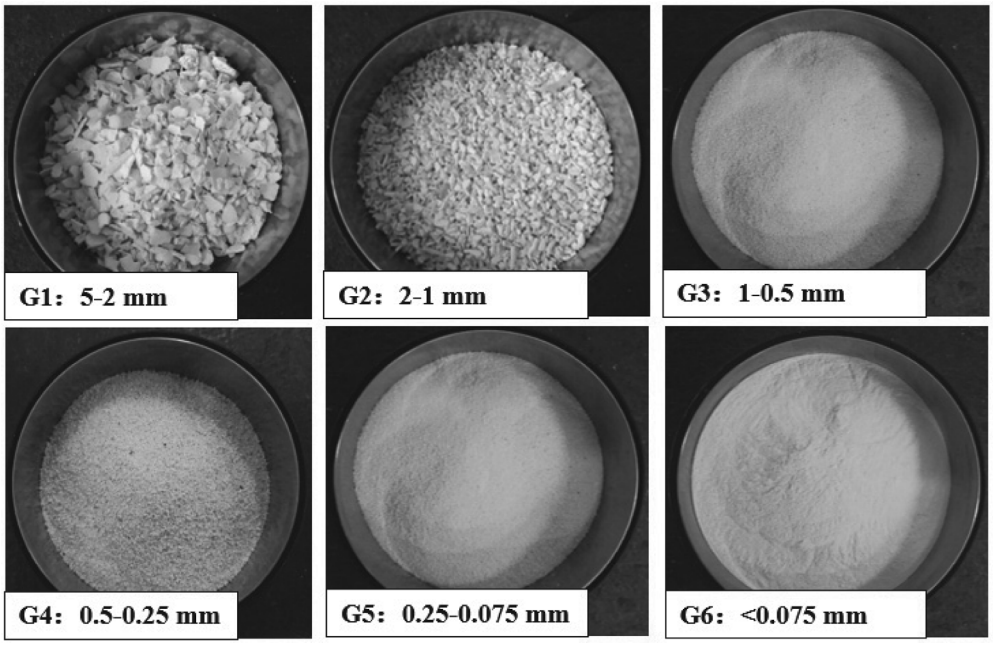

Figure 1. Original calcareous sand particles with different size groups.

Table 1. Basic physical properties of calcareous sand.

Size groups	G1	G2	G3	G4	G5	G6
G_s	2.790	2.791	2.792	2.795	2.801	2.811
ρ_{max} (g/cm^3)	1.131	1.000	1.047	0.999	1.303	1.442
ρ_{min} (g/cm^3)	0.678	0.683	0.743	0.747	0.925	1.045

ing behaviour in stress-strain response and a contraction behaviour in volumetric strain. Furthermore, for the samples with particle size ranging from 0.25 to 0.075 mm (G5 sand), a strain hardening behaviour is triggered by an effective confining pressure of 800 kPa, which is more than 200 kPa for the samples with particle size ranged from 5 (G1 sand) to 0.25 mm (G4 sand). This indicates that the effective confining pressure corresponding to a strain softening-hardening transition increases with the increase in particle size, which is further supported by the fact that the samples with particle size smaller than 0.075 mm (G6 sand) still demonstrate a strain softening behaviour under the effective confining pressures of 800 kPa. Similar results can also be found in Wang et al. (2018). This phenomenon is caused by the difference in particle breakage, dependent on the particle size, and is explained as follows. The sample with larger particles having lower particle crushing strength can be crushed easily under a low effective confining pressure, which increases the deviatoric stress and leads to a strain hardening behaviour. For the samples with smal-

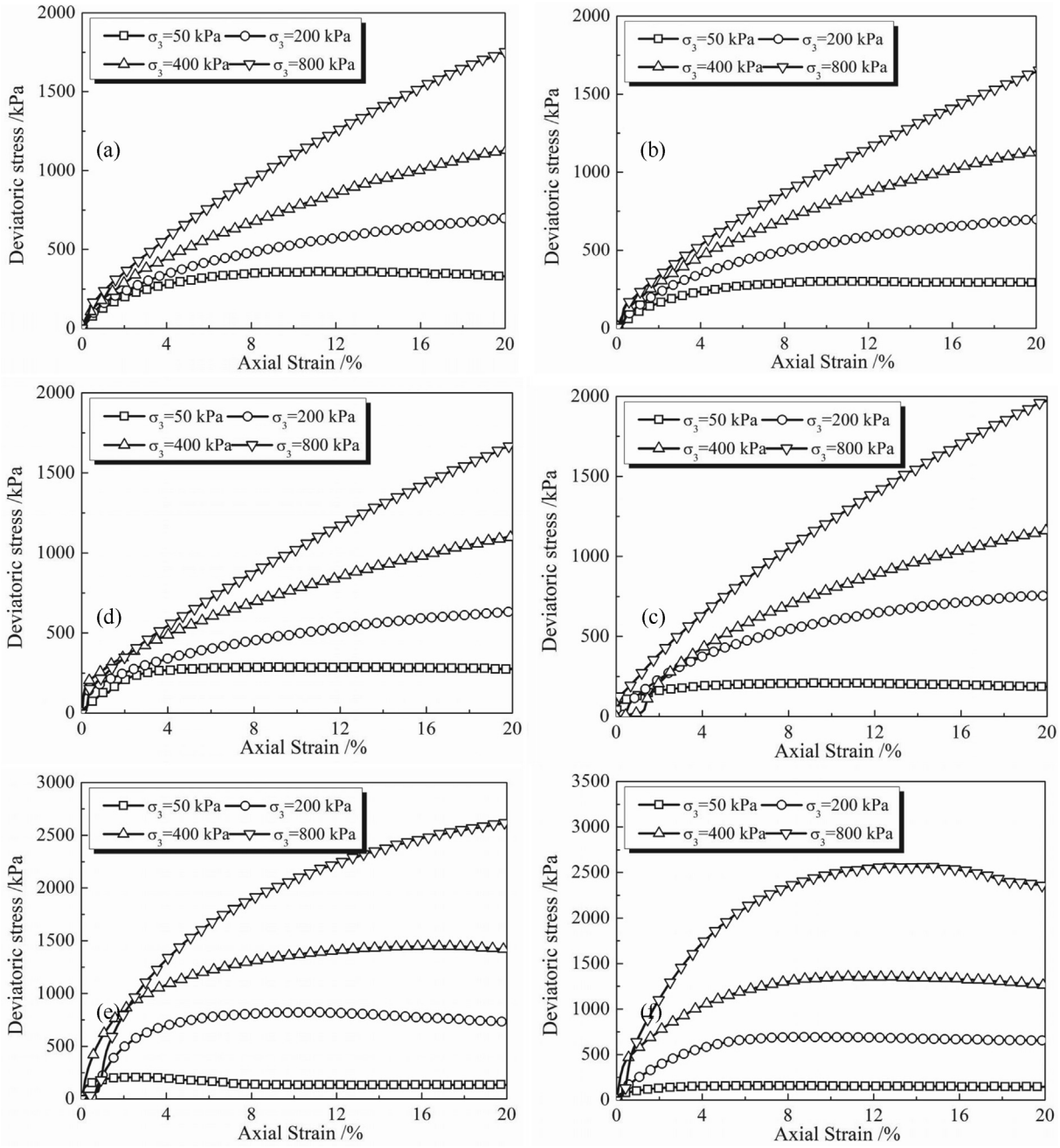

Figure 2. Stress-strain responses for different particle sizes: (a) G1: 5-2 mm, (b) G2: 2-1 mm; (c) G3: 1-0.5 mm, (d) G4: 0.5-0.25 mm, (e) G5: 0.25-0.075 mm, (f) G6: < 0.075 mm.

ler particles, the effective confining pressure corresponding to a strain softening-hardening transition increases owing to the contributions of higher particle crushing strength.

The relationships between the shear peak strength and particle size under various effective confining pressures are shown in Figure 3. It is apparent from Figure 3 that the shear peak strength of calcareous sand under different effective confining pressures depends on the particle size. The shear peak strength decreases with the decreasing particle size under the effective confining pressure of 50 kPa. However, under relatively large effective confining pressure ($\sigma_3 \geq 200$ kPa), the shear peak strength increases with the decreasing particle size. In addition, the shear peak strength of samples with small particles is more susceptible to the effective confining pressure upon increasing particle crushing strength compared to samples with large particles, so that there is a significant increase in the peak shear strength for effective confining pressures higher than 400 kPa for groups G5 and G6.

3.2 Effect of particle size on volumetric responses

Figure 4 presents the volumetric responses of calcareous sand samples with different particle sizes under various effective confining pressures. In Figure 4, the volumetric strain is positive for contraction. Experimental observations show that the dense calcareous sand samples are more likely to exhibit volumetric contraction behaviour under high effective confining pressure. Furthermore, a higher effective confining pressure produces a larger volumetric contraction. There is a higher probability for the calcareous sand particles to break under higher effective confining pressure, which reduces the volumetric dilatancy. However, at a low effective confining pressure ($\sigma_3 = 50$ kPa), the samples with particle size ranged from 5 (G1 sand) to 1 mm (G2 sand) demonstrate slight volumetric contraction at a relatively large axial strain, which is considered to be produced by the particle breakage induced by the increasing deviatoric stress during shearing.

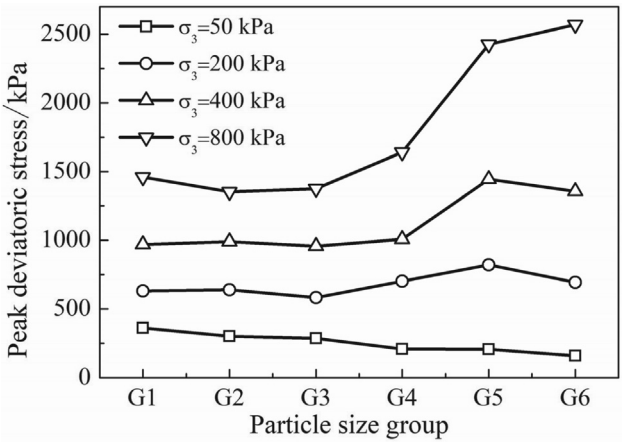

Figure 3. Relationships between shear peak strength and particle size.

3.3 Effect of particle size on apparent cohesion and friction angle

Traditionally, shear strength of granular materials is represented by the Mohr-Coulomb failure criterion, which can be expressed as follows:

$$\tau = c + \sigma_n \tan\phi \tag{1}$$

where τ is the shear strength of the sample; c is the apparent cohesion; σ_n is the normal stress on shear plane; ϕ is the friction angle.

According to the Mohr-Coulomb failure criterion, both the apparent cohesion and the friction angle for all samples with different particle sizes were obtained. Figure 5 illustrates the relationships between the Mohr-Coulomb strength index and particle size. Obviously, both the apparent cohesion and the friction angle are strongly dependent on the particle size, which is in accordance with the experimental results reported by Wang et al. (2018), shown in Figure 5. Generally, the quartz sand is considered to be non-cohesive, exhibiting a friction angle of about 30°. However, the calcareous sand samples have a high apparent cohesion which decreases with the decreasing particle size. As calcareous sands consist of corals, shells, and alga, the particle shapes are columnar, dendritic, honeycomb, or sheet (Shahnazari et al., 2016; Wang et al., 2018). Therefore, grain interlocking between coarse particles behaves as apparent cohesion in shearing. Besides, as stated by Wang et al. (2018), the large calcareous sand particle is more irregular and angular in shape than the smaller calcareous sand particle, leading to a higher apparent cohesion. For the samples with particle size less than 0.075 mm (G6 sand), the apparent cohesion is almost zero, indicating that the shear strength is more likely to be supplied by the friction component rather than the cohesion component. Besides, it is also can be seen that the friction angle increases with the decreasing particle size.

3.4 Effect of particle size on strain softening and dilatancy

In order to further analyse the softening behaviour of calcareous sand with different particle sizes, the empirical softening index is proposed, which can be calculated as follows:

$$\beta = \frac{q_p - q_r}{q_p} \tag{2}$$

where q_p is the shear peak strength, q_r is the reference strength, which is taken as the deviatoric stress corresponding to an axial strain of 20 %, as shown in Figure 6. For the strain-stress responses exhibiting a strain hardening behaviour, q_p and q_r are taken as the deviatoric stress corresponding to an axial strain of 15 % and 20 %, respectively. Based on definition of the empirical softening index, the samples

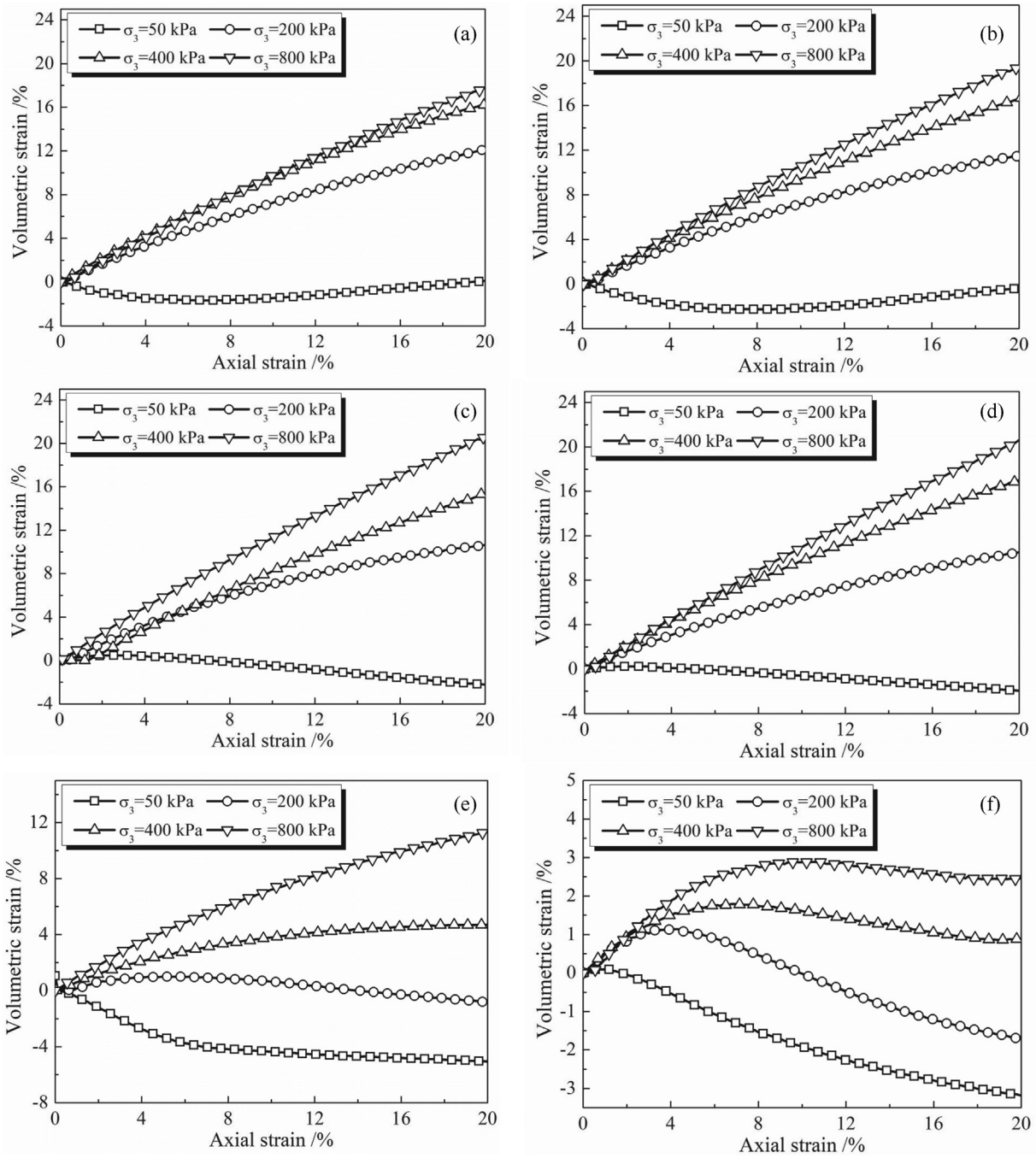

Figure 4. Volumetric responses for different particle sizes: (a) G1: 5-2 mm, (b) G2:2-1 mm, (c) G3: 1-0.5 mm, (d) G4: 0.5-0.25 mm, (e) G5: 0.25-0.075 mm, (f) G6: < 0.075 mm.

exbibit a strain softening behaviour with $\beta > 0$, whereas the samples exbibit a strain hardening behaviour with $\beta \leq 0$.

The relationships between the empirical softening index and confining pressure for different particle sizes are illustrated in Figure 7 on a semi-logarithmic scale. Significant linear relationships were obtained between the empirical softening index and the effective confining pressure for different particle sizes, which could be expressed as $\beta = k_\beta \log(\sigma_3) + b_\beta$. For the samples with particle size ranged from 5 (G1 sand) to 0.075 mm (G5 sand), the empirical softening index decreases with the increasing effective confining pressure, implying that the strain softening behaviour is more obvious under a lower effective confining pressure. In addition, it is also can be found that the strain softening behaviour is slightly influenced by the effective confining pressure for the samples with particle size less than 0.075 mm (G6 sand).

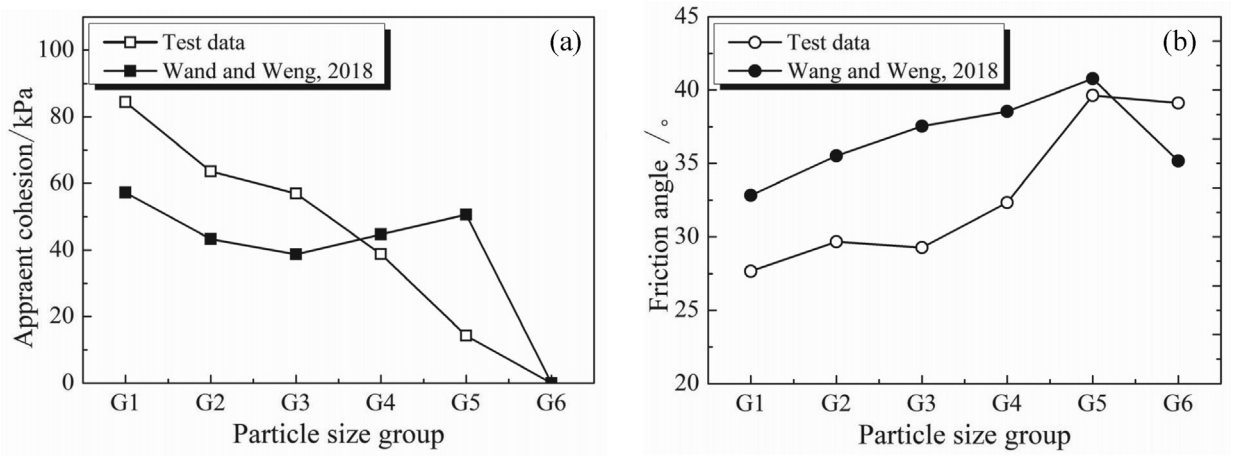

Figure 5. Relationships between Mohr-Coulomb strength index and particle size: (a) apparent cohesion, (b) friction angle.

An empirical dilatancy index is also proposed to evaluate the dilatancy behaviour quantificationally. The empirical dilatancy index is defined as:

$$\xi = \frac{\varepsilon_{vc} - \varepsilon_{vp}}{\varepsilon_{qc} - \varepsilon_{qp}} \tag{3}$$

where ε_{vc} is the volumetric strain at $d\varepsilon_v^p / d\varepsilon_q^p = 0$, with $d\varepsilon_v^p$ being the increment of volumetric plastic strain and $d\varepsilon_q^p$ being the increment of axial plastic strain. ε_{vp} is the volumetric strain corresponding to the shear peak strength. ε_{qc} and ε_{qp} are the axial strain corresponding to ε_{vc} and ε_{vp}, respectively. Based on the definition, the samples exbibit a volumetric contraction behaviour continuously with $\xi \geq 0$, whereas the samples exhibit a volumetric dilatancy behaviour with $\xi < 0$. The corresponding values of four parameters (*e.g.*, ε_{vc}, ε_{vp}, ε_{qc}, and ε_{qp}) mentioned above for different types of volumetric responses are shown in Figure 8. Note that both the ε_{vc} and ε_{qc} are assumed to be zero for the type D volumetric response.

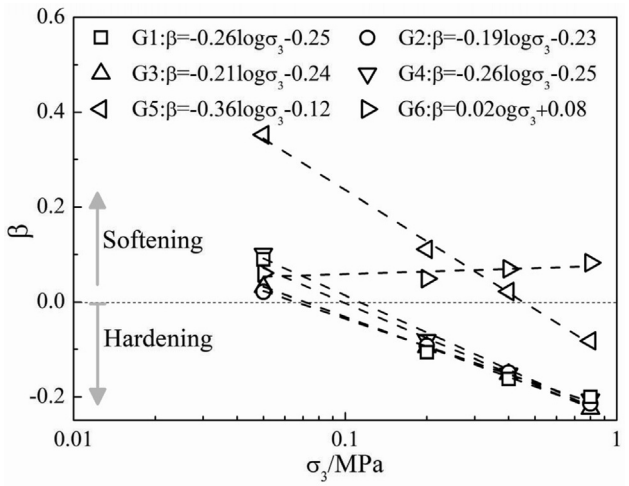

Figure 7. Relationships between empirical softening index and effective confining pressure for different particle sizes.

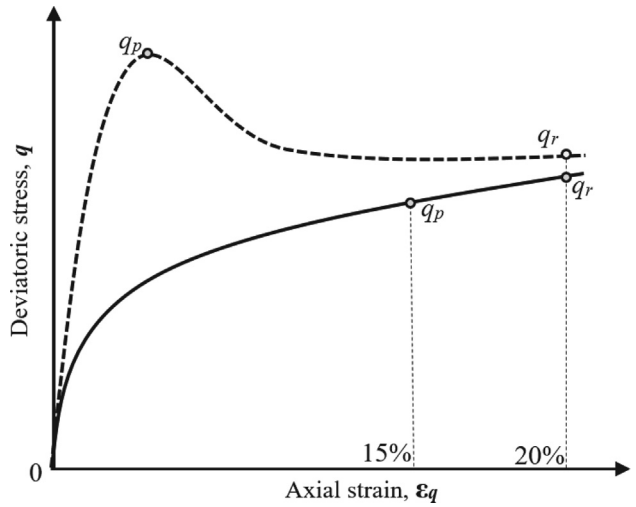

Figure 6. Representation of the empirical softening index.

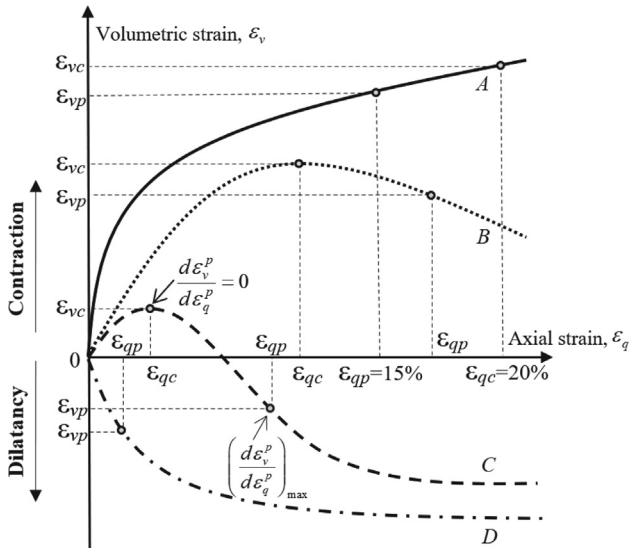

Figure 8. Representation of the empirical dilatancy index.

Figure 9 shows the relationships between the empirical dilatancy index and the effective confining pressure for different particle sizes. As shown in Figure 9, the empirical dilatancy indexes are linearly related to the effective confining pressures in semi-logarithmic scale, which can be described by $\xi = k_\xi \log(\sigma_3) + b_\xi$. It is found that the empirical dilatancy index for different particle sizes increases with the increasing effective confining pressure, indicating that the volumetric dilatancy behaviour is suppressed by the increasing effective confining pressures. For calcareous sand, the particle breakage has a significant influence on the volumetric behaviour (Bandini & Coop, 2011; Shahnazari et al., 2014; Shahnazari et al., 2015). It seems that both a higher effective confining pressure and a larger particle size can lead to a larger extent of particle breakage, which reduces the volumetric dilatancy (Wang et al., 2018; Shahnazari et al., 2015). It can be concluded that the volumetric behaviour of calcareous sand sample is the result of synergy of particle breakage and dilatancy (Wang et al., 2018). In addition, for G6 sand, the samples exhibit a volumetric dilatancy behaviour under various effective confining pressures.

4. Conclusions

To investigate the effect of particle size on mechanical properties of calcareous sand, a series of consolidated drained triaxial tests were performed on calcareous sand with different particle sizes. The test results indeed reveal the effect of particle size on the shear behaviour of dense calcareous sands. The following main conclusions are drawn from the present study:

(1) The shear peak strength, the apparent cohesion, and the friction angle are all dependent on the particle size. At a low effective confining pressure of 50 kPa, the shear peak strength increases with the increasing particle size. However, under a relatively large effective confining pressure (≥ 200 kPa), the shear peak strength decreases with the increasing particle size. Moreover, the apparent cohesion increases, and the corresponding friction angle decreases with the increase of particle size.

(2) The high effective confining pressure may lead to strain hardening behaviour for dense calcareous sand samples, corresponding to contraction in volumetric strain. The softening and dilatancy indexes were proposed to evaluate the softening and dilatancy behaviour quantitatively. Calcareous sands with larger particle size showed the greater strain hardening and volumetric contraction behaviour, which is more susceptible to the effective confining pressure.

(3) In order to further investigate the particle size effect of shear behaviour of dense calcareous sands, a comprehensive analysis should be combined with the microstructure of calcareous sands. In addition, it is also worthwhile to explore the engineering characteristics of calcareous sands with different gradations under complex stress conditions.

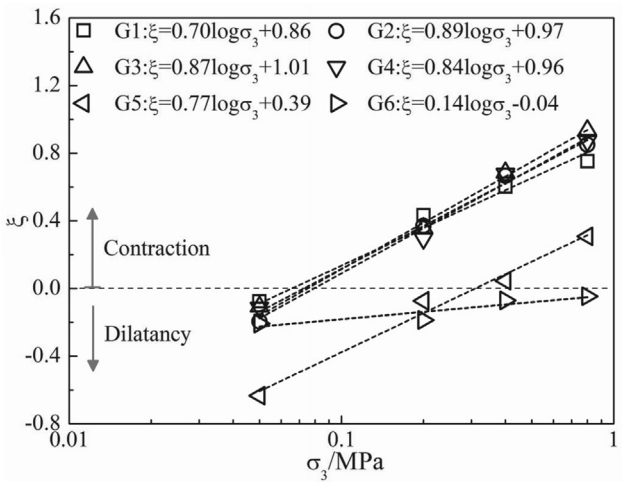

Figure 9. Relationships between empirical dilatancy index and effective confining pressure for different particle sizes.

Acknowledgments

This research was supported by the National Natural Science Foundation of China (Grant Nos. 51971188 and 51071134), the Science and Technology Major Project of Hunan Province (Grant No. 2019GK1012), Huxiang High-Level Talent Gathering Program of Hunan Province-Innovative team (Grant No. 2019RS1059) and the Degree and Postgraduate Education Reform Project of Hunan Province (Grant No. CX20190493). All these supports are acknowledged.

References

Bandini, V., & Coop, M.R. (2011). The influence of particle breakage on the location of the critical state line of sands. *Soils and Foundations*, 51(4), 591-600. https://doi.org/10.3208/sandf.51.591

Coop, M.R., Sorensen, K.K., Bodas Freitas, T.M., & Georgoutsos, G. (2004). Particle breakage during shearing of a carbonate sand. *Geotechnique*, 54(3), 157-163. https://doi.org/10.1680/geot.2004.54.3.157

Dadkhah, R., Ghafoori, M., Ajalloeian, R., & Gholam, R.L. (2010). The effect of scale direct shear test on the strength parameters of clayey sand in Isfahan City, Iran. *Journal of Applied Sciences*, 10(18), 2027-2033.

Desrosiers, R., & Silva, A.J. (2002). Strength behavior of marine sands and elevated confining stresses. *Marine Georesources and Geotechnology*, 20(1), 1-19. https://doi.org/10.1080/106411902753556834

Hyodo, M., Hyde, A.F.L., & Aramaki, N. (1998). Liquefaction of crushable soils. *Gl otechnique*, 48(2), 527-543. https://doi.org/10.1680/geot.1998.48.4.527

Liu, L., Liu, H.L., Stuedlein, A.W., Evans, M.T., & Yang, X. (2019). Strength, stiffness, and microstructure char-

acteristics of biocemented calcareous sand. *Canadian Geotechnical Journal*, 56(10), 1502-1513. https://doi.org/10.1139/cgj-2018-0007

Lade, P.V., Liggio, C.D., & Nam, J. (2009). Strain rate, creep, and stress drop-creep experiments on crushed coral sand. *Journal of Geotechnical and Geoenvironmental Engineering*, 135(7), 941-53. https://doi.org/10.1061/(ASCE)GT.1943-5606.000006

Morsy, A.M., Salem, M., & Elmamlouk, H.H. (2019). Evaluation of dynamic properties of calcareous sands in Egypt at small and medium shear strain ranges. *Soil Dynamics and Earthquake Engineering*, 116, 692-708. https://doi.org/10.1016/j.soildyn.2018.09.030

Mcdowell, G.R., & Bolton, M.D. (2000). Effect of particle size distribution on pile tip resistance in calcareous sand in the geotechnical centrifuge. *Granular Matter*, 2(4), 179-187. https://doi.org/10.1007/PL00010913

RIOH JTG E40-2007. (2007). Test methods of soils for highway engineering. *RIOH - Research Institute of Highway Ministry of Transport*, Beijing, China.

Shahnazari, H., Jafarian, Y., Tutunchian, M.A., & Rezvani, R. (2016). Undrained cyclic and monotonic behavior of hormuz calcareous sand using hollow cylinder simple shear tests. *International Journal of Civil Engineering*, 14(4), 209-219. https://doi.org/10.1007/s40999-016-0021-6

Shahnazari, H., Rezvani, R., & Tutunchian, M.A. (2015). An experimental study on the phase transformation point of crushable and noncrushable soil. *Marine Georesources and Geotechnology*, 35(2), 176-85. https://doi.org/10.1080/1064119X.2015.1126773

Shahnazari, H., Salehzadeh, H., Rezvani, R., & Dehnavi, Y. (2014). The effect of shape and stiffness of originally different marine soil grains on their contractive and dilative behavior. *KSCE Journal of Civil Engineering*, 18(4), 975-83. https://doi.org/10.1007/s12205-014-0286-8

Suescun-Florez, E., & Iskander, M. (2017). Effect of fast constant loading rates on the global behavior of sand in triaxial compression. *Geotechnical Testing Journal*, 40(1), 52-71. https://doi.org/10.1520/GTJ20150253

Salehzadeh, H., Procter, D., & Merrifield, C.M. (2006). Medium dense non-cemented carbonate sand under reversed cyclic loading. *International Journal of Civil Engineering*, 4(1), 54-63.

Wang, X.Z., Jiao, Y.Y., Wang, R., Hu, M.J., Meng, Q.S., & Tan, F.Y. (2011). Engineering characteristics of the calcareous sand in Nansha Islands, South China Sea. *Engineering Geology*, 120(4), 40-47. https://doi.org/10.1016/j.enggeo.2011.03.011

Wang, X., Zhu, C.Q., Wang, X.Z., & Qin, Y. (2018). Study of dilatancy behaviors of calcareous soils in a triaxial test. *Marine Georesources and Geotechnology*, 37(9), 1507-1070. https://doi.org/10.1080/1064119X.2018.1526236

Wei, H.Z., Zhao, T., Meng, Q.S., Wang, X.Z., & He, J.Q. (2018). Experimental evaluation of the shear behavior of fiber-reinforced calcareous sands. *International Journal of Geomechanics*, 18(12), 04018175. https://doi.org/10.1061/(ASCE)GM.1943-5622.0001307

Wen, R., Tan, C., Wu, Y., & Wang, C. (2018). Grain size effect on the mechanical behavior of cohesionless coarse-grained soils with the discrete element method. *Advances in Civil Engineering*, 2018, 4608930-1-6. https://doi.org/10.1155/2018/4608930

Wang, Y., Zhou, L., & Yang, Q. (2019). Hydro-mechanical analysis of calcareous sand with a new shape-dependent fluid-particle drag model integrated into CFD-DEM coupling program. *Powder Technology*, 344, 108-120. https://doi.org/10.1016/j.powtec.2018.12.008

Wang, X.Z., Weng, Y.L., Wang, X., & Chen, W.J. (2018). Interlocking mechanism of calcareous soil. *Rock and Soil Mechanics*, 39(9), 3113-3120 (In Chinese).

Giang, P.H.H., Van Impe, P.O., Van Impe, W.F., Menge, P., Cnudde, V., & Haegeman, W. (2017). Effects of particle characteristics on shear strength of calcareous sand. *Acta Geotechnica Slovenica*, 14(2), 77-89.

Varadarajan, A., Sharma, K.G., Venkatachalam, K., & Gupta, A.K. (2003). Testing and modeling two rockfill materials. *Journal of Geotechnical and Geoenvironmental Engineering*, 129(3), 206-218. https://doi.org/10.1061/(ASCE)1090-0241(2003)129:3(206)

Xiao, Y., Yuan, Z., Chu, J., Liu, H., Huang, J., Luo, S.N., & Lin, J. (2019) Particle breakage and energy dissipation of carbonate sands under quasi-static and dynamic compression. *Acta Geotechnica*, 14(6), 1741-1755. https://doi.org/10.1007/s11440-019-00790-1

Xiao, P., Liu, H.L., Xiao, Y., Stuedlein, A.W., & Evans, T.M. (2018). Liquefaction resistance of bio-cemented calcareous sand. *Soil Dynamics and Earthquake Engineering*, 107, 9-19. https://doi.org/10.1016/j.soildyn.2018.01.008

Yang, S., Zhu, Y.H., Liu, H.L., Li, A., & Ge, H.Y. (2018). Macro-meso effects of gradation and particle morphology on the compressibility characteristics of calcareous sand. *Bulletin of Engineering Geology & the Environment*, 77, 1047-1055. https://doi.org/10.1007/s10064-017-1157-6

Zhang, X., Hu, W., Scaringi, G., Baudet, B.A., & Han, W. (2018). Particle shape factors and fractal dimension after large shear strains in carbonate sand. *Gotechnique Letters*, 8(1), 73-79. https://doi.org/10.1680/jgele.17.00150